High Capacity 64-Quadrature Amplitude Modulation Based Optical Coherent Transceiver for 60 GHz Radio Over Fiber System

Devendra Chack
   Indian Institute of Technology (Indian School of Mines): Indian Institute of Technology

SUNIL NARAYAN THOOL (✉ sunilthool.18dp000388@ece.iitism.ac.in)
   Indian Institute of Technology (Indian School of Mines): Indian Institute of Technology
   https://orcid.org/0000-0001-9423-9183

High Capacity 64-Quadrature Amplitude Modulation based Optical Coherent Transceiver for 60 GHz Radio Over Fiber System

Devendra Chack[1], and Sunil N. Thool[1]

[1] Department of Electronics Engineering, Indian Institute of Technology (ISM), Dhanbad, Jharkhand-826004, India

Abstract Today's world demands for maximum bandwidth utilization in the area of optical fiber network to achieve serious progress due to data consumption has been grown by > 25% as compared to last year. 5G system is one of the promising technology cater for high bandwidth utilization between multiple transceivers and have the advantages to operate in the milli-meter wave (mm-wave) of 60 GHz. There is much interest of photonic technique such as optical heterodyne coherent detection to produce mm-wave frequencies. We propose a 60 GHz radio over fiber (RoF) link using 168 Gb/s high capacity input data rate based 64-Quadrature amplitude modulation (64-QAM), coherent detection using optical heterodyning and advanced digital signal processing (ADSP) based system. An optimized version of optical heterodyne technique is used to derive 60 GHz radio frequency (RF) signal for connecting radio nodes over wireless link. In order to compensate the irregularities effect of standard signal mode fiber (SSMF), a novel ADSP technique is used which allows good improvement in the spectral signal efficiency and achieved longer distance communication. The ADSP technique plays a key role to achieve high capacity data rate requirements for forthcoming 5G technologies. The proposed RoF system shows that an error free transmission is accomplished over 170 km SSMF and achieved BER is 2.7×10^{-3} against 7.015 % error vector magnitude (EVM) with 30 dB Signal to Noise ratio (SNR).

Keywords: **Optical Communication, Radio over fiber (RoF), Coherent Detection, Advanced DSP, 5G**

I. INTRODUCTION

We are in an era of 5G, Internet of things (IoT), virtual reality and Distributed Data Centre, are used to provide the higher data transmission to facilitated the end user needs such as high definition (HD) video communication to enhanced the interconnectivity across the world. In order to address these requirements and to accommodate the exponential growth of huge bandwidth generated by new networking standards, it is essential to upgrade the existing and current data transmission scheme used in optical communication and wireless data transmission system. IEEE 802.11ad is a 60 GHz wireless networking standard used to provide multigigabit data transmission [1]. A 60 GHz V-band can be used to transmit the data at high data rate and enabling the usage to transmit the uncompressed video over wireless channel for shorter distance communication. Hence, it is now becoming more popular and replacement solution for the conventional Wireless Fidelity (Wi-Fi) system [2] and to be used in upcoming 5G technologies [3]. A 60 GHz mm-wave is an imminent and most suitable option for rapidly increasing huge bandwidth requirements in broadband wireless communication for forthcoming 5G technologies. Due to the limitation of 60 GHz performance and a huge loss in the air transmission, still it is found to be a most suitable solution for indoor communication for high-speed data transmission in unlicensed spectrum, e.g. HD video transmission [4]. A recent development in the optical fiber-based RoF cater for unlimited bandwidth capabilities and invulnerability of electromagnetic interference becomes a most popular [5]. Hence, it is used for long-haul transmission with a large data payload. The RoF system mainly consists of central station (CS), where the baseband signal processing and conversion of modulating signal into optical followed by transmission over longer distance SSMF to the Base station (BS) is carried out. Today's wireless communication needs to be highly stable and spectrally efficient to fully utilize available spectrum bandwidth. M-ary QAM shows its higher spectral efficiency as compared to the other modulations like binary phase-shift keying (BPSK), amplitude shift keying (ASK) and quadrature phase-shift keying (QPSK). Hence, m-ary QAM is widely used in mm-wave wireless access systems. However, in QAM as the order of m-ary increases with lower symbol rates shows better spectral signal efficiency, and when it is transmitted over optical fiber, the effect of dispersion reduces effectively and hence, m-QAM shows more potential for high capacity data rate transmission over long haul RoF link [6]-[13].

Although many research papers reported that the mm-wave RoF wireless communication systems realized several tens of gigabyte signal transmission, it is limited to a shorter distance and used a higher radio frequency (RF) band.
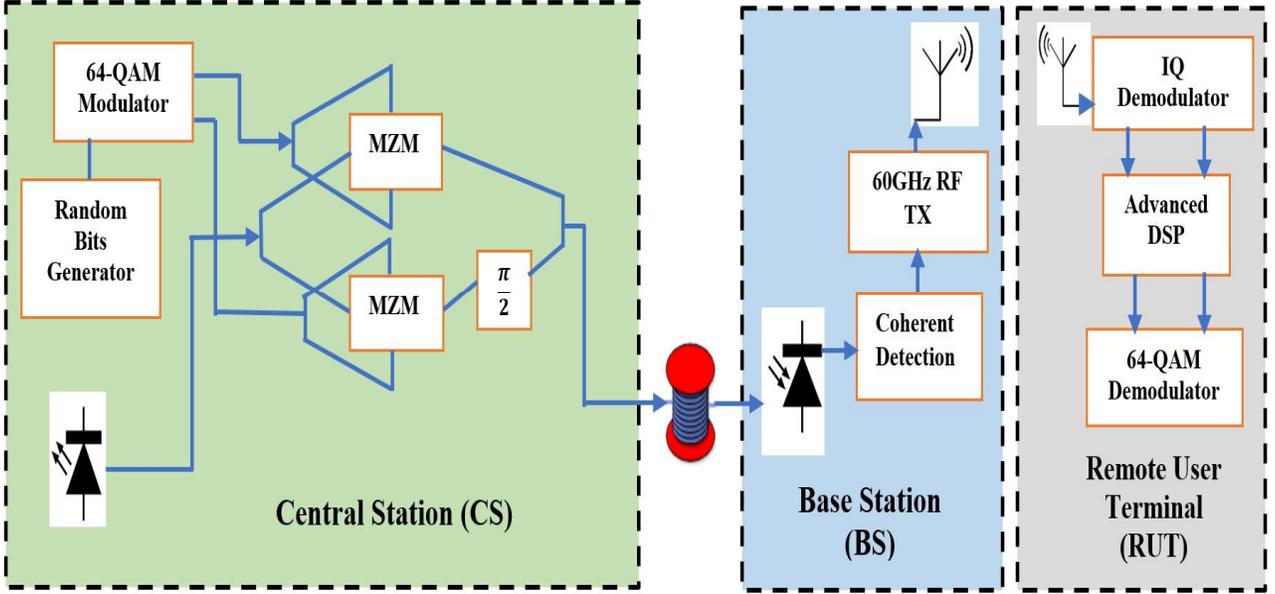
Figure. 1. Proposed 60 GHz mm-wave RoF system, 64-QAM (Quadrature Amplitude modulator), LiNbO3-MZM (Mach-Zander Modulator), π/2 = 90º Phase shift, IQ (In-phase and Quadrature Demodulator), Advanced DSP (Digital Signal Processing)

But, it had encountered with many technical challenges as mentioned in references [6]-[17]. Among all the major challenges, a very important and crucial challenge is to combat the fiber's loss due to its dispersive nature. Hence, to reduce the fiber dispersion an optical single sideband (SSB) based modulation and 90º hybrid couplers are used in optical modulation system. Similarly, high precise biasing is applied to the optical modulator. A sharp roll-off optical filter increases the spectral signal efficiency of the optical signal significantly to transmit over SSMF. Phase noise contribution by free running continuous wave (CW) laser would be responsible to increase the complexity in DSP at the receiver system for carrier phase noise estimation [18].

In this paper, we propose a RoF link cater for 168 Gb/s input data rate modulated baseband signal using 64-QAM and transmitted over SSMF, a 60 GHz mm-wave RF signal generation using optical heterodyning coherent detection and ADSP technique is depicted in Fig 1. The baseband In-Phase(I) and Quadrature(Q) component of 64-QAM signal is optically modulated using two orthogonal arms of LiNbO3 Mach–Zehnder modulator (LiNbO3-MZM). The CW laser is tune with 193.4144 THz at central station (CS). An optical signal is intercepted by optical heterodyning coherent detection method and converted into 60 GHz RF signal at base station (BS) with CW laser tune with 193.3544 THz. The generated 60 GHz RF signal is transmitted over wireless link to connect various radio user terminal (RUT). The 60 GHz RF is received by RUT and further it is demodulated by IQ demodulator.

The IQ demodulator consists of 60 GHz local oscillator (LO) signal generator, mixer and low pass filter (LPF). The received noisy RF signal is mixed with LO and passed through the LPF, which has cut off frequency $0.2\times$ data rate to reduce the intermodulation products generated during the mixing process. The noise contaminated baseband 64-QAM received signal is passed through ADSP, which consist of filtering, resampling, IQ imbalance compensation, chromatic dispersion (CD) and fiber non liner (NL) effect compensation. It is also consisting of timing recovery to compensate the delay, adaptive equalization for desired symbol trajectory recovery, down-converter to convert signal with same sample per symbol rate desired at base band level. Carrier Phase estimation (CPE) and Frequency Offset estimation (FOE) is used to eliminate phase and frequency deviation encountered while transmission through fiber. The obtained results are discussed as symbol error rate (SER), bit error rate (BER), constellation diagrams, EVM %, and received optical signal power at various distances of optical fiber varies from 150 km to 172 km.

This paper is prepared as, in section II, the principle of operation is discussed for the proposed RoF system with technical background of optical heterodyning coherent detection and ADSP techniques. Section III, describes the proposed simulation setup, its implementation, results and design of RoF system and finally conclusion has been drawn in section IV.

II. PRINCIPLE OF OPERATION OF ROF LINK

The system design, implementation, and analysis are carried for the proposed optical links as shown in Fig.2 and fiber impairments combat using advanced DSP techniques and shown in Fig. 3.

$$E_{equ}(t) = \gamma_1 \gamma_2 \, E_0 J_2(m_h) \left\{ \exp j(\omega_0 + 2\omega_{RF})t + \frac{\pi}{V_\pi} [I(t) + jQ(t)] \exp j(\omega_0 + 2\omega_{RF} + \omega_{IF})t \right\} \quad (2)$$

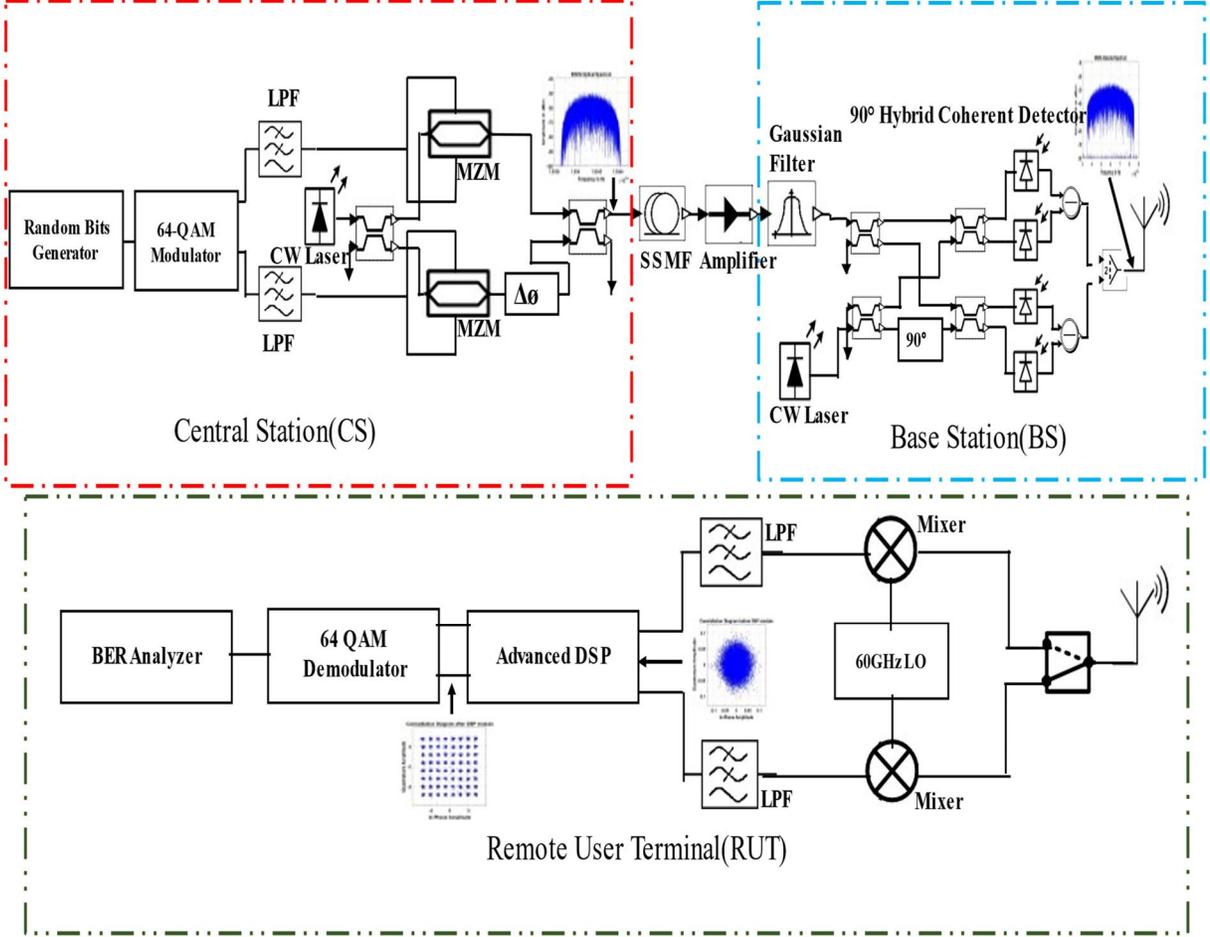γ_1, γ_2 is insertion loss of MZM.

Figure 2. Proposed 60 GHz RoF link

Note: The system design, implementation and analysis are carried for optical link and its impairments combat using advanced DSP.

A CW laser diode running at fundamental frequency $f_0 = 2\pi/\omega_0$ and emitted light waves $E_0(t) = E_0 \exp(j\omega_0 t)$. The baseband I and Q signals are modulated with light wave generated by laser source via two arms based orthogonal LiNbO3-MZM. The biasing voltages of LiNbO3-MZM is optimized to modulate the I and Q signal. The baseband I and Q signals of 64-QAM is represented as,

$$S(t) = I(t) \sin\omega_{RF} t + Q(t) \cos\omega_{RF} t \quad (1)$$

The SSB modulation using MZM modulator configured with bias voltages of $\frac{V_\pi}{2}$ and phase difference of $\frac{\pi}{2}$.

The modulation index is chosen as $\alpha = \pi I(t)/V_\pi$ and $\beta = \pi Q(t)/V_\pi$. The SSB optical modulated signal is represented as,

This $E_{equ}(t)$ generated at CS and transmitted though SSMF with dispersion factor and nonlinear irregularities with standard attenuation factor. The mm-wave optical signal at BS is detected using high speed photo diode with optical heterodyning coherent detection technique. The photo current flow thorough PD consist of mm-wave RF signal including dc components.

The baseband modulating signal and carrier signal is expressed as,

$$I(t) = \mu \gamma_1^2 \gamma E_0^2 J_2^2(m_h) \left\{ 1 + \gamma_2^2 + \gamma_2^2 \frac{\pi^2}{V_\pi^2} [I^2(t) + Q^2(t)] + 2\gamma_2 \cos4\omega_{RF} t + 2\gamma_2 \frac{\pi}{V_\pi} [I(t) \cos(4\omega_{RF} + \omega_{IF})t + Q(t) \sin(4\omega_{RF} + \omega_{IF})t + 2\gamma_2^2 [I(t) \cos\omega_{IF}(t) + Q(t) \sin\omega_{IF}(t) \right\} \quad (3)$$

μ is the sensitivity of photo diode.

The optical heterodyne coherent detection for the 64-QAM is realized with 2×2 and 90º optical hybrid for converting the phase information into optical intensity equivalent. The generated optical signal is passed through the balanced detector (BD) using high speed photo detector converts the optical signal into I and Q signals [16],[17]. The electrical I and Q signal combine using combiner to get 60 GHz RF signal. The operating frequency for coherent detection CW laser source is selected with 60 GHz frequency offset with respect to CW laser operating frequency of optically modulated 64-QAM transmitted signal.

The 60 GHz RF signal is radiated to connect the different RUTs over a wireless link. The RUTs are intercepted the 60 GHz RF and then passed through IQ demodulators and generate 64-QAM baseband signal which is highly contaminated by noise, the non-linear effect of optical fiber medium, phase noise effect of channel etc. The baseband signal is passed through the ADSP comprises different techniques starting with a preprocessing step followed by the signal recovery at the final stage. In the preprocessing stage the received signal is passed through the fiber channel characteristics of Samples/Symbol = (C) x Samples per bit. This process also contains the DC blocking and normalization of the signals. where C is a constant and its value depends on the modulation scheme used. The ADSP technique is realized with sequences blocks as shown in Fig 3.

A. Bessel Filter, Resampling and IQ Compensation

The received RF signal at RUT is contaminated by transmission channel bandwidth noise added with optical sampled signal. The extra DC shift caused by voltages applied to the modulators is compensated by DC blocking third order Bessel Filter better shaping factor, flatter phase delay, and flatter group delay. The output of Bessel Filter is passed through the resampling process at a rate of 2 samples/symbol.
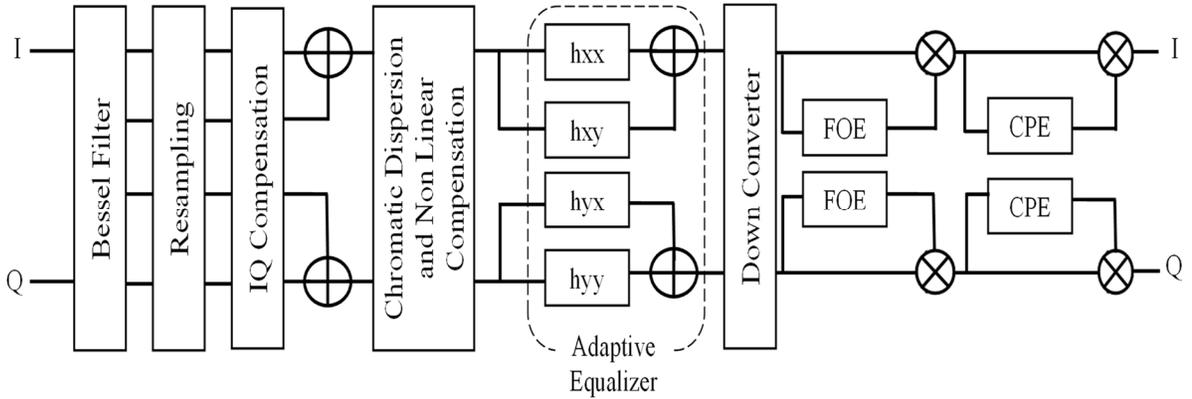
through fiber, to mitigate this, IQ compensation block is used. It is realized with Gram-Schmidt orthogonalization procedure (GSOP). The I-Q components of the received signal, denoted by r I (t) and r Q (t). The GSOP generated orthonormal signals are represented by Io(t) and Qo(t),

$$I^0(t) = \frac{r_1(t)}{\sqrt{P_1}}$$

$$Q' = r_Q(t) - \frac{\rho.r_1(t)}{\sqrt{P_1}} \tag{4}$$

$$Q^0(t) = \frac{Q'(t)}{\sqrt{P_Q}}$$

$\rho = E\ \{r\ I(t),\ r\ Q\ (t)\}$ is the correlation coefficient;
$P\_I = E\ \{r2I(t)\};\ P\_Q = E\ \{Q'2(t)\}.$

B. Chromatic Dispersion, Non-Linear Compensation and Timing Recovery

In the proposed implementation, digital filtering is used to compensate chromatic dispersion of optical fiber. A frequency domain and time domain filters are implemented [19]. The frequency domain transfer function is depicted as,

$$G(z, \omega) = \exp\left(-j.\frac{D.\lambda^2.z}{4.\pi.c}.\omega^2\right) \tag{5}$$

where z, ω, λ, c, S, and λo are transmission distance, angular frequency, wavelength, speed of light, dispersion slope, reference wavelength respectively. The dispersion coefficient of the fiber is represented as $D = Do + S\ x\ (\lambda - \lambda o)$. Similarly, the time domain implementation using N taps, finite impulse response filter (FIR) is used for CD compensation.

Figure 3. Advanced DSP techniques blocks

The resampling of I-Q signals has been carried out using a cubic interpolation method. The down sampling is also used to convert the up-sampled signal to their original rate of 4 × samples per bit after equalization process. The I-Q signal is imbalanced in amplitude and phase while passing

The tap weights for FIR are represented in eq. (6)

$$a_k = \sqrt{\frac{j.c.T^2}{D.\lambda^2 \times z}}.exp\left(-j.\frac{\pi.c.T^2}{D.\lambda^2.z}.k^2\right) \tag{6}$$

$$-\left\lfloor \frac{N}{2} \right\rfloor \le k \le \left\lfloor \frac{N}{2} \right\rfloor$$

$T = \pi/\omega.$ ω_n is the Nyquist frequency.

A digital back propagation is used to reduce nonlinear compensation [19]. A back propagation (BP), inverse nonlinear Schrödinger equation (NLSE) is used to solve optical link parameter. The NLSE is represented as,

$$\frac{\partial E}{\partial(-z)} = (D + N)E \tag{7}$$

D and N are the differential operator, the nonlinear operator, complex received signal E is given by,

$$D = \frac{j}{2} \cdot \beta_2 \cdot \frac{\partial^2}{\partial t^2} \frac{\alpha}{2} \tag{8}$$

$$N = j\gamma|E|^2$$

β_2 is dispersion parameter group velocity, α is the attenuation factor and γ is the nonlinearity parameter. As per the explanation given in [20],[21] a Split-Step Fourier method (SSFM) is used to solve the above Eq. (7), (8). The phase shifts for each sample are calculated by Eq. (9),

$$\theta_{NL}(t) = k\gamma L_{eff}|E|^2 \tag{9}$$

where k is a compensation factor, effective length of each step is represented by L_{eff}. In case of more than one fiber spans, it is then compensated by each BP step. Then, the effective L_{eff} is represented as,

$$L_{eff} = s \cdot \frac{1 - \exp(-\alpha L_{span})}{\alpha} \tag{10}$$

where S and L_{span} is the number of fiber spans and length of each span respectively.

The exact and correct time of samples and symbols are adaptively determined by timing recovery algorithm. Sampling frequency and sampling phase may be change due to oscillator frequency drift stated for specific symbol rate as well as the filter process introduced a timing delay. The timing recovery algorithm is implemented by digital square and filter algorithm.
The received signal is written as,

$$r(t) = \sum_{k=-\infty}^{\infty} a_k \cdot g_t \cdot [t - k.T - \varepsilon(t).T] + n(t) \tag{11}$$

where a_k are the transmitted symbols, $g\ T(t)$, $n(t)$ is the transmission signal and channel noise respectively. T is the symbol duration. ε is a time delay which varies slowly. The received signal is passed through the filter sampled at a rate of $4/T$, resulting as shown under,

$$\tilde{r}(t) = r(t) \otimes g_R(t) \tag{12}$$

$$\tilde{r}k = \tilde{r}. \frac{KT}{4} \tag{13}$$

The sequence:
$$x_k = \left| \sum_{m=-\infty}^{\infty} a_m \cdot g\left(\frac{KT}{4} - m.T - \varepsilon.T\right) + \right.$$
$$\left. \tilde{n} \cdot \left(\frac{KT}{4}\right) \right|^2 \tag{14}$$

$g(t) = g_t((T) \otimes g_R(T)$ represents the filtered samples and squared input signal. This spectral component at 1/T is determined for every section of the length of the signal. At last signal is computed using complex Fourier coefficients at the symbol rate and is represented as,

$$X_n = \sum_{k-4nL}^{4(n+1)LN-1} x_k e^{-\frac{j2\pi k}{4}} \tag{15}$$

The normalized phase

$$\hat{\varepsilon} = -\frac{1}{2.\pi} \cdot \arg(x_n) \tag{16}$$

is an unbiased estimate for ε.

C. Adaptive Equalizer (AE)

An adaptive equalizer (AE) is used to reduce the residual chromatic dispersion, polarization mode dispersion (PMD) and inter-symbol interference. The AE is implemented by using two stage Constant modulus algorithm- radius directed (CMA-RD) algorithm. The CMA cost function is given by,

$$J(k) = E\left[(|y(k)|^2 - R_p)^2\right] \tag{17}$$

In this case the cost function used as,

$$J(k) = E\left[(|y(k)|^2 - R_p)^2\right] - |E[y(k)^2]|^2 \tag{18}$$

The second term forces the equalizer to be non-circularly symmetric [22]. For equations (17) and (18), $y(k)$ equalizer output and $E[...]$ is the statistical expectation. Rp depending on the input data symbol $a(k)$ with dispersion order p and it is represented as,

$$R_p = \frac{E[|a(k)|^{2p}]}{E[|a(k)|^p]} \tag{19}$$

The equalizer output $y(k)$ is obtained from

$$y(k) = W^H.X(k) \tag{20}$$

$$W = [w_0(k), w_1(k) \dots w_{N-1}(k)]^T \tag{21}$$

$$X_k = [x_0(k), x_1(k-1), \dots x_{N-1}(k-N+1)]^T \tag{22}$$

where W, $X(k)$ and N are the equalizer input, weights of equalizer tap, length of the equalizer tap weights respectively. The tap weights vector is represented by,

$$W_{(k+1)} = W(k) + \mu.X(k).e^*(k) \tag{23}$$

$$e(k) = y(k).(R_p - |y(k)|^2) \tag{24}$$

The stochastic gradient algorithm is used to calculate the weight vector. $e(k)$ is the error signal and μ is the step size parameter. The error signal is calculated as,

$$e(k) = y(k).\left(R_p - |y(k)|^2\right) + \frac{|y(k)|^2 y^*(k)}{2} \tag{25}$$

For a 64-QAM signal, fine tune equalization is carried out by CMA for first order convergence and followed by RD algorithm as error $e(k)$. The equalizer output and the nearest constellation optimization is done by RD. The error for RD is,

$$e(k) = y(k).\left(\widehat{R_k^P} - |y(k)|^p\right) \tag{26}$$

where R_k is the radius of the nearest constellation symbol for each equalizer output. The updated tap weights for the RD as,

$$W(k+1) = W(k) + \mu.X(k).e^*(k) \tag{27}$$

$$e(k) = \widehat{R_k^P} - |y(k)|^p \tag{28}$$

A large data sample is required to get a good result. Therefore, we use multiple iterations are attempted to adopt the tap weights.

D. Frequency Offset Estimation (FOE) and Carrier Phase Estimation (CPE)

The mixing of received signal with the local oscillator frequency generated intermodulation product and also deviates the frequency and phase components which leads to a symbol rotating constellation. The received signal with carrier and phase offset is represented by,

$$S(k) = C(k).e^{j(2\pi\Delta fkT + \varphi_k)} + n(k) \tag{29}$$

where $C(k)$, Δf and φk are data symbols, frequency offset and carrier phase respectively. For 64-QAM the modulation information cannot be removed by 6th power, therefore $S^6(k)$ is described as,

$$S^6(k) = A.e^{j.6.(2\pi\Delta fkT + \varphi_k)} + e(k) \tag{30}$$

$$A = E[C_6 6] \tag{31}$$

where A and $e(k)$ are amplitude and a zero-mean noise respectively. The frequency offset estimation is based on the max. spectral density of a signal $S^6(k)$ as given by,

$$S^6(k) = \frac{1}{6} arg\{max[|Z(f)|]\} \tag{32}$$

$$Z(f) = \frac{1}{N}\sum_{k=0}^{N-1} S^6(k)e^{-j(2\pi fkT)} \tag{33}$$

In order to recover the phase and remove phase mismatch, the blind phase search (BPS) algorithm [23] is used. The optimum value is determined by using BPS algorithm uses different test phases. The received signal Zk is rotated by B test carrier phase angles φ_b, given as,

$$\varphi_b = \frac{b}{B}.\frac{\pi}{2} \quad \text{with } b\in \{0,1,\ldots\ldots.B-1\} \tag{34}$$

All received symbols are passed through the decision unit. and squared distance between the symbols $|dk,b|^2$ is calculated as,

$$\left|d_{k,b}\right|^2 = \left|Z_k e^{j\varphi b} - \widehat{X_{k,b}}\right|^2 \tag{35}$$

where $X_{k,b}$ is the decision of $Z_k e^{j\varphi b}$.

An averaging method is used to mitigate the effect of the noise. It is considered as the N symbols block have same phase noise. The summation of such N consecutive test symbols by the same carrier phase angle φ_b is represented as,

$$S_{k,b} = \sum_{n=1}^{N} |d_{k-n.b}|^2 \tag{36}$$

The laser line-width symbol duration product affects optimum value of N. The switch-controlled index *mk*, min of the minimum distance sum is decoded the output symbol X_k selected from $X_{k,b}$. Linear interpolation is used to improve the performance for the phase noise components which varies rapidly. 64- QAM constellation mapping is calculated by unwrapping after phase noise to remove 6-pole ambiguity.

III. PROPOSED 60 GHZ MM-WAVE ROF SIMULATION SETUP, RESULTS AND DISCUSSION

The proposed implementation of 60 GHz mm-wave RoF link is verified in optisystem, and obtained results are analyzed in the Matlab. A CW laser is tuned at the frequency wavelength of 1550 nm (193.4144 THz) with a linewidth of 10 MHz. A CW laser acts as a light source of LiNbO3-MZM modulator at CS. The optical spectrum of 64-QAM is shown in Fig. 4.
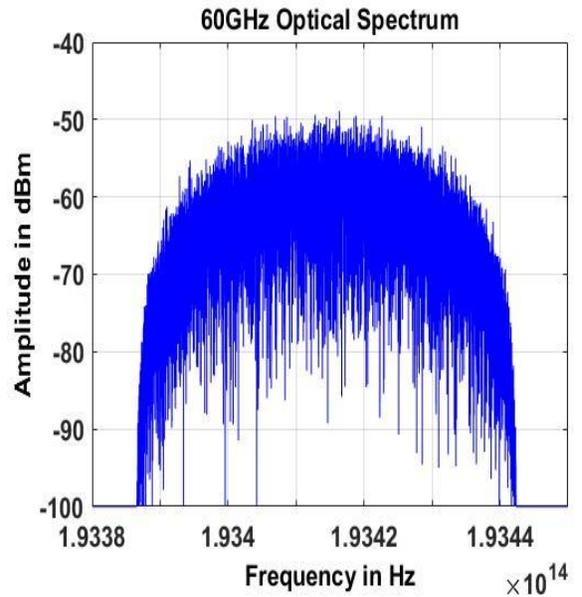

Figure 4. Optical Spectrum 64-QAM Signal.

The amplitude of the 64-QAM optical spectrum is -50 dBm due to loss incurred in the modulation process. An optical amplifier is used to compensates it with gain of 20 dB. The SSMF with a dispersion of 16.75 ps/nm/km and insertion loss (IL) of 0.2 dB/km is used to transmit the optical signal at maximum distance of 172 km. The variable optical power amplifier compensates the IL of SSMF to normalize the amplitude of the received signal at a distance of 172 km. At the base station, the optical signal is intercepted by high-speed photodiode based optical heterodyne coherent detection, where 60 GHz spacing CW laser tune at a frequency of 1550.48 nm (193.3544 THz). The coherent detection output generates a 60 GHz RF signal. This 60 GHz RF is transmitted over a wireless link to connect RUTs. The detected RF signal spectrum of 60 GHz signal at BS propagatedover170 km fiber length is shown in Fig.5.
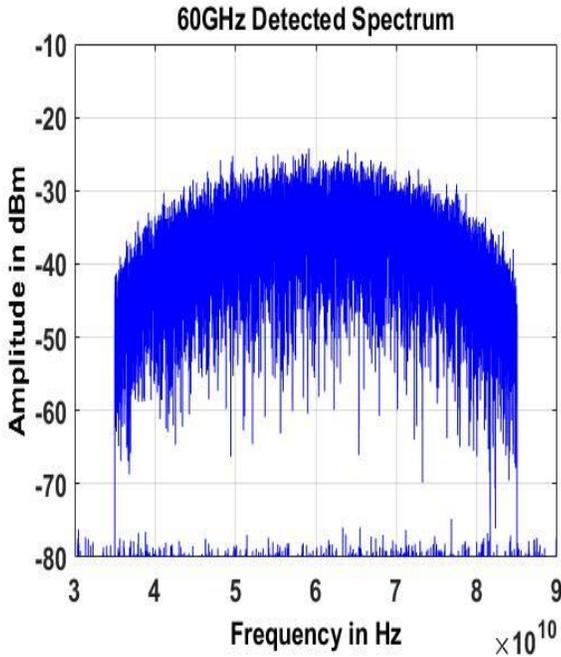

Figure 5. 60 GHz RF signal detection using optical heterodyning Coherent detection

It is observed that -30 dBm RF signal is detected at 170 km fiber. This signal is further transmitted at the RUT. The RUT consists of IQ demodulator in which mixing of LO with 60 GHz received RF is mixed using electrical mixer and further, it is passed through LPF with cut off frequency 0.2×data rate. The received baseband 64-QAM signal prior to ADSP is represented with constellation diagram as shown in Fig. 6 and Fig. 7 at the fiber length 172 km and 150 km respectively. The constellation diagram indicates that the phase mismatch of the symbol trajectory is due to different optical and RF channel factors as discussed in section-II. In order to mitigate these, an ADSP blocks are used. The ADSP block realized with various techniques and algorithms as discussed in section-II. The 64-QAM constellation diagram after ADSP block is shown in Fig.6 and Fig. 7 for same fiber lengths.

The constellation diagrams results show significant improvement in the symbol trajectory after passing through

ADSP block which is incorporated by chromatic dispersion compensation, IQ imbalance compensation, channel equalization and FOE, CPE over 172 km to 150 km optical fiber lengths.
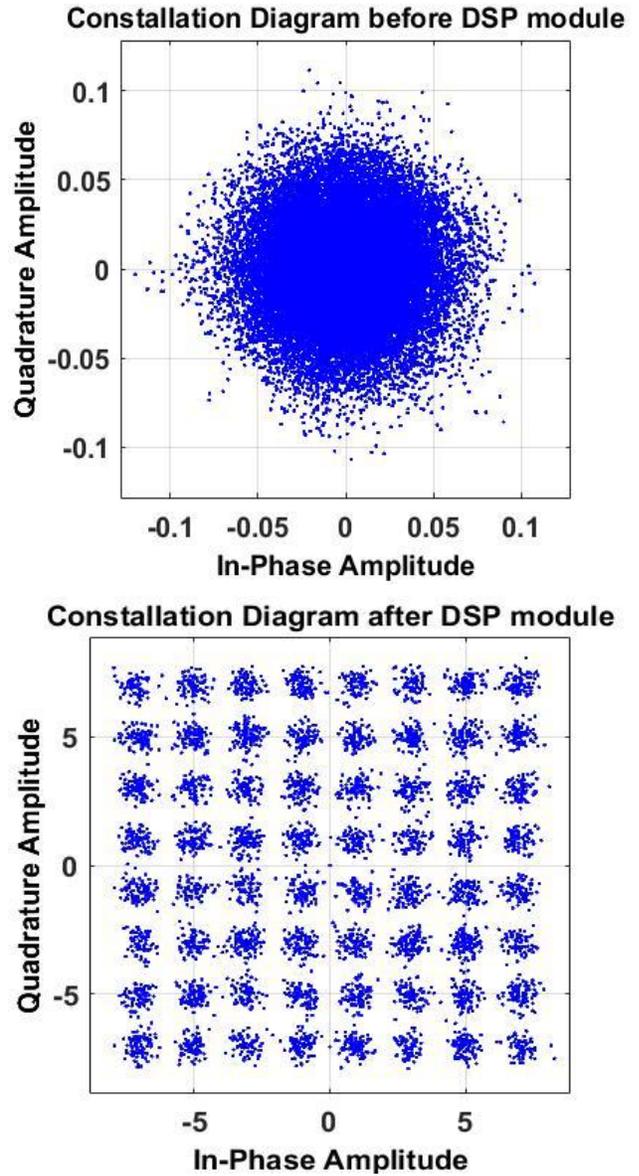

Figure 6. Constellation Diagram before and after ADSP at optical fiber length of 172 km

The post received signal after ADSP is passed through the 64-QAM demodulator with 6 Bits/symbol setting and converted into digital bits stream and finally EVM and BER calculation is carried out. The Error vector magnitude of the baseband signal and is calculated form constellation diagram using following eq.

$$EVM(\%) = \sqrt{\frac{\sum n|\hat{x}n - a_x^{opt}x_n|^2 + |\hat{y}n - a_x^{opt}y_n|^2}{\sum n|a_x^{opt}x_n|^2 + |a_x^{opt}y_n|^2}} \qquad (37)$$

This equation represents n^{th} symbol of I-Q signal $\hat{x}n$ and $\hat{y}n$ respectively. Similarly, x_n and y_n are the input symbols

and a_x^{opt} and a_{xy}^{opt} are the optimized attenuation coefficient of I-Q signal level and calculated as, $a_x^{opt} = \langle \frac{\hat{x}n}{xn} \rangle$ and $a_{xy}^{opt} = \langle \frac{\hat{y}n}{yn} \rangle$ and mean of variation is calculated for transmitted and received symbols.
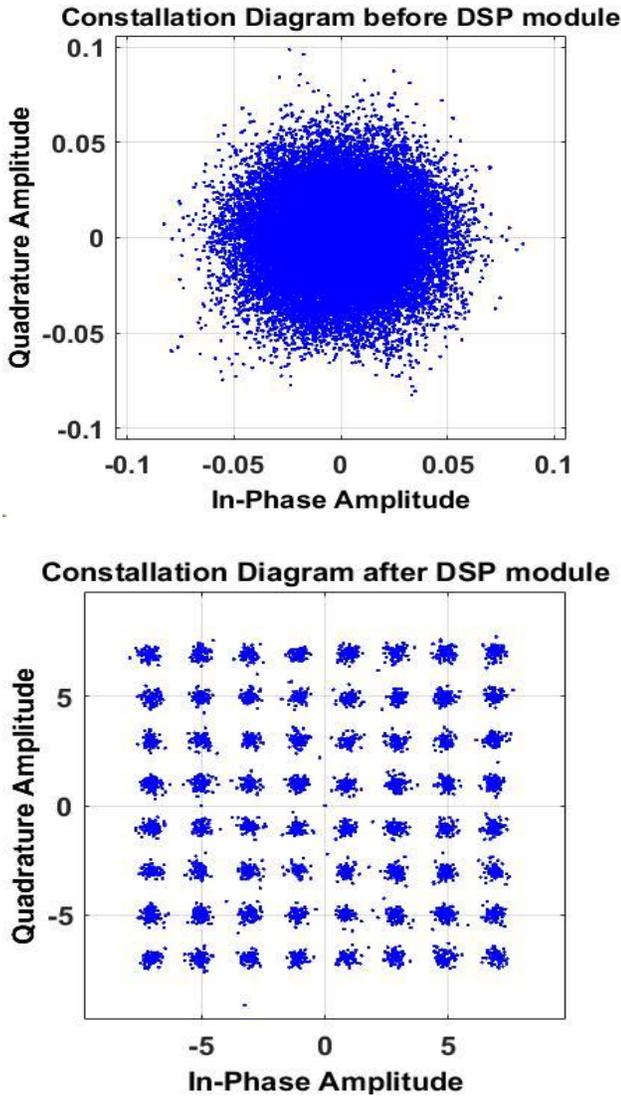

Figure. 7. Constellation Diagram before and after ADSP at optical fiber length of 150 km

The EVM is observed as 7.015% against the received power of 7.886 dBm at the end of SSMF and input of optical heterodyne coherent detection module i.e., at BS and eventually it is reduced with reduction into fiber length from 172 km to 150 km. At 150 km EVM is 1.006% against the received power of 8.35 dBm. The EVM % vs received power plot is shown in the Fig. 8 and the received power vs fiber length is shown in Fig. 9. The logarithmic BER between the received bit stream and input bitstream is calculated using BER analyzer and represented in Fig. 10. According to the BER curve, it is seen that BER 2.7×10^{-3} is achieved with this novel RoF scheme at fiber length of

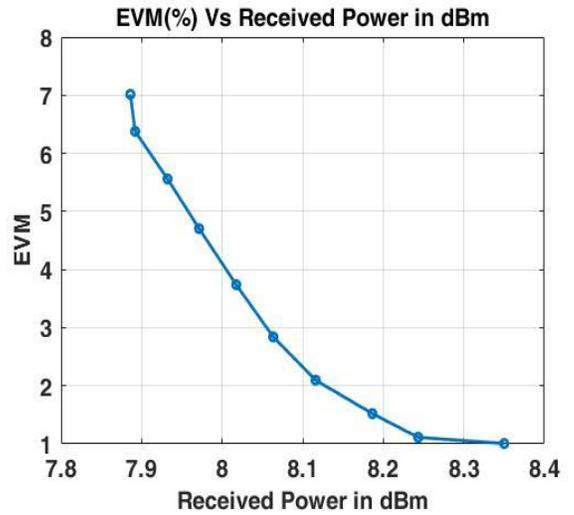170 km which is more reliable and suitable for long haul communications.

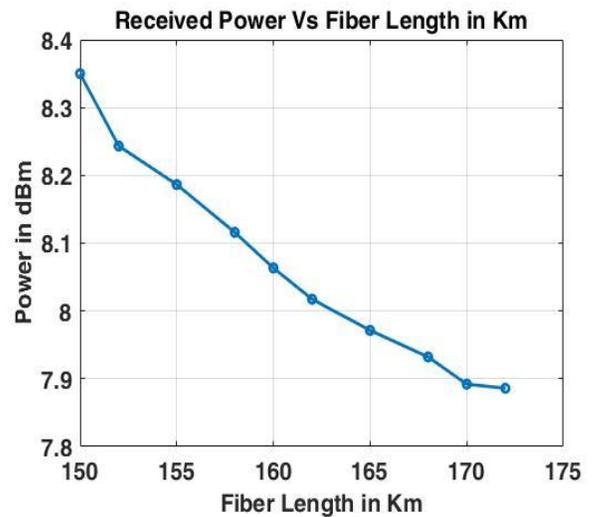Figure 8. Received Power Vs EVM rms in (%)

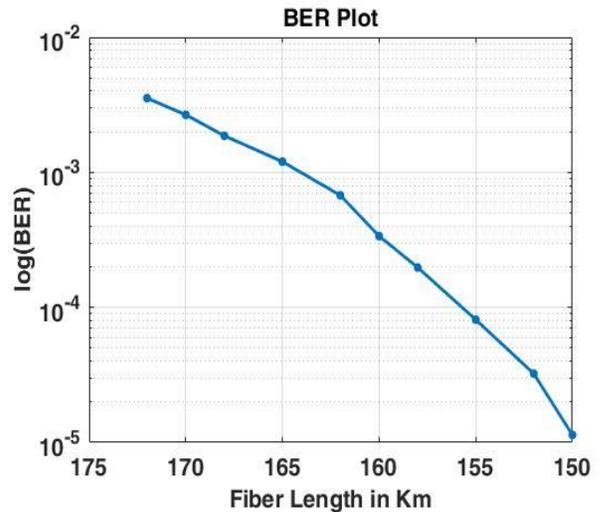Figure 9. Optical Fiber length Vs Received power

Figure 10. Optical Fiber length in km Vs logarithmic BER plot

Parameters/ Ref no.	Ref [6][y] 2016	Ref. [9][y] 2010	Ref. [12][y] 2016	Ref. [14][y] 2017	Ref. [15][x] 2011	Proposed Implementation
Input Data Rate	120 Gbps	112.8 Gbps Dual Polarization	1 Gbaud	60 Gbps	480/240 Mbps Up/Down Link	168 Gbps
Modulation Scheme	64-QAM	64-QAM	64-QAM	64-QAM	64-QAM	64-QAM
DSP Unit	--	--	Yes	--	--	Advanced DSP
Fiber Length/OSNR	60 km	26.5 dB (OSNR)	--	20 km	10 km	170 km
BER	3.8×10^{-3}	2×10^{-3}	2×10^{-2}	2×10^{-2}	-	2.7×10^{-3}
EVM	--	--	--	--	2.3%	7.015%
Heterodyne Coherent Detection	--	Yes	Yes	--	Yes	Yes

x – simulation results, y- experimental results

Table-1 Comparison of pervious implementation with proposed 60 GHz RoF using 64-QAM.

Table-1 highlights the comparison on the implementation of 60 GHz RoF system using 64-QAM. According to the comparison, it is observed that the proposed implementation is supported for longer distance communication by using ADSP technique over the larger SSMF distance upto 170 km with 2.7×10^{-3} BER. This proposed scheme also increases a significant amount of bandwidth utilization for high payload data transmission over longer distance of optical fiber with EVM well below its limit of < 7.015%.

IV. CONCLUSION

The proposed 60 GHz mm-wave RoF implementation using 168 Gb/s, 64-QAM, in which the optical signal generation is done with dual-arm based orthogonal optical modulator and generates spectrally efficient signal at CS. The RF link between BS and RUT is achieved using high-speed photodiode-based optical heterodyne coherent detection where 60 GHz RF signal generation occurs. The RUT is realized with I-Q demodulator and ADSP module, responsible for reconstructing the baseband 64-QAM signal trajectory. The analysis of signal through constellation diagrams, EVM and BER observed by the simulation results to recover the signal at a distance of 170 km optical fiber. The proposed RoF link represents its superior performance which is more suitable for ultra-wide bandwidth and high capacity data rate requirements for forthcoming 5G technologies and also fulfill the long-distance optical communication needs.

DISCLOSURE STATEMENT
No potential conflict of interest was reported by the authors.

REFERENCES

[1] "IEEE Standard for Information technology--Telecommunications and information exchange between systems--Local and metropolitan area networks--Specific requirements-Part 11: Wireless LAN Medium Access Control (MAC) and Physical Layer (PHY) Specifications Amendment 3: Enhancements for Very High Throughput in the 60 GHz Band," in IEEE Std 802.11ad-2012 (Amendment to IEEE Std 802.11-2012, as amended by IEEE Std 802.11ae-2012 and IEEE Std 802.11aa-2012) , vol., no., pp.1-628, 28 Dec. 2012, doi: 10.1109/IEEESTD.2012.6392842.

[2] Nitsche, Thomas & Cordeiro, Carlos & Flores, Adriana & Knightly, Edward & Perahia, Eldad & Widmer, Joerg. (2014). IEEE 802.11ad: directional 60 GHz communication for multi-Gigabit-per-second Wi-Fi [Invited Paper]. Communications Magazine, IEEE. 52. 132-141. 10.1109/MCOM.2014.6979964.

[3] L.Vallejo, B.Ortega, D.-N. Nguyen, J. Bohata, V. Almenar and S. Zvanovec, "Usability of a 5G Fronthaul Based on a DML and External Modulation for M-QAM Transmission Over Photonically Generated 40 GHz," in IEEE Access, vol. 8, pp. 223730-223742, 2020, doi: 10.1109/ACCESS.2020.3042756.

[4] C. Lim, Y. Tian, C. Ranaweera, T. A. Nirmalathas, E. Wong and K. Lee, "Evolution of Radio-Over-Fiber Technology," in Journal of Lightwave Technology, vol. 37, no. 6, pp. 1647-1656, 15 March15, 2019, doi: 10.1109/JLT.2018.2876722.

[5] Zhenzhou Tang, Fangzheng Zhang, Shilong Pan," 60-GHz RoF System for Dispersion-Free Transmission of HD and Multi-Band 16QAM", IEEE Photon. Technol. Lett., vol. 30, no. 14, pp. 1305-1308, Jun.(2018).

[6] X. Li, Y. Xu and J. Yu, "Over 100-Gb/s V-Band Single-Carrier PDM-64QAM Fiber-Wireless-Integration System," in IEEE Photonics Journal, vol. 8, no. 5, pp. 1-7, Oct. (2016).

[7] H. Zhang, A. Wen, W. Zhang, W. Zhang, W. Zhai and Z. Tu, "A Novel Spectral-Efficient Coherent Radio-Over-Fiber Link with

Linear Digital-Phase Demodulation," in IEEE Photonics Journal, vol. 12, no. 1, pp. 1-8, Feb. (2020).

[8] X. Li and J. Yu, "Generation and Heterodyne Detection of >100-Gb/s Q -Band PDM-64QAM mm-Wave Signal," in IEEE Photonics Technology Letters, vol. 29, no. 1, pp. 27-30, 1 Jan.1, (2017).

[9] Yu, X. Zhou, S. Gupta, Y. Huang and M. Huang, "A Novel Scheme to Generate 112.8-Gb/s PM-RZ-64QAM Optical Signal," in IEEE Photonics Technology Letters, vol. 22, no. 2, pp. 115-117, Jan.15, (2010).

[10] T. Rahman et al., "Long-Haul Transmission of PM-16QAM-, PM-32QAM-, and PM-64QAM-Based Terabit Super Channels Over a Field Deployed Legacy Fiber," in Journal of Lightwave Technology, vol. 34, no. 13, pp. 3071-3079, 1 July1, (2016).

[11] P. Torres-Ferrera, S. Straullu, S. Abrate and R. Gaudino, "Upstream and downstream analysis of an optical fronthaul system based on DSP-assisted channel aggregation," in IEEE/OSA Journal of Optical Communications and Networking, vol. 9, no. 12, pp. 1191-1201, Dec.(2017).

[12] Dong, "64QAM Vector Radio-Frequency Signal Generation Based on Phase Precoding and Optical Carrier Suppression Modulation," in IEEE Photonics Journal, vol. 8, no. 6, pp. 1-7, Dec. (2016).

[13] J. Ma, Y. Zhan, M. Zhou, H. Liang, Y. Shao and C. Yu, "Full-duplex radio over fiber with a centralized optical source for a 60 GHz millimeter-wave system with a 10 Gb/s 16-QAM downstream signal based on frequency quadrupling", Opt. Commun. Netw., vol. 4, no. 7, pp. 557-564, Jul. (2012).

[14] X. Li, J. J. Yu, Y. M. Xu, et al., "60-Gbps W-band 64QAM RoF system with T-spaced DD-LMS equalization," Proc. Opt. Fiber Commun. Conf. Exhib. (OFC), pp. 1 -3, Mar. (2017).

[15] S. Ghafoor and L. Hanzo, "Sub-Carrier-Multiplexed Duplex 64-QAM Radio-over-Fiber Transmission for Distributed Antennas," in IEEE Communications Letters, vol. 15, no. 12, pp. 1368-1371, December (2011).

[16] C.-K. Weng, Y.-M. Lin, and W.-I. Way, "Radio-over-fiber 16-QAM, 100-km transmission at 5 Gb/s using DSB-SC transmitter and remote heterodyne detection," J. Lightwave Technol., vol. 26, no. 6, pp. 643–653, Mar. 2008

[17] Z. Tang and S. Pan, "A full-duplex radio-over-fiber link based on a dual-polarization Mach–Zehnder modulator", IEEE Photon. Technol. Lett., vol. 28, no. 8, pp. 852-855, Apr. (2016).

[18] S. J. Savory, "Digital filters for coherent optical receivers", Optics Express, Vol. 16, No. 2, Jan.21 (2008).

[19] Liang B. Du and Arthur J. Lowery, "Improved single channel back propagation for intra-channel fiber nonlinearity compensation in long-haul optical communication systems", Optics Express, vol. 18, no. 16, pp. 17075-17088, (2010).

[20] K. Kikuchi, M. Fukase, and S.-Y. Kim, "Electronic post-compensation for nonlinear phase noise in a 1000-km20-Gbit/s optical QPSK transmission system using the homodyne receiver with digital signal processing," Optical Fiber Communication Conference (Optical Society of America, Anaheim, California, 2007), p. OTuA2.

[21] A. J. Lowery, "Fiber nonlinearity mitigation in optical links that use OFDM for dispersion compensation," IEEE Photon. Technol. Lett. 19(19), 1556-1558 (2007).

[22] E. Pincemin et. al., "Novel Blind Equalizer for Coherent DP-BPSK Transmission Systems: Theory and Experiment", IEEE Photon. Tech. Lett., V25, pp 1835 (2013).

[23] T. Pfau, S. Hoffmann, and R. Noe, "Hardware-Efficient Coherent Digital Receiver Concept with Feed-forward Carrier Recovery for M-QAM Constellations", Journal of Lightwave Technology, Vol. 27, No. 8, pp. 989-999, Apr 15 (2009).